



# Electric Field and Space Charge Distribution in Propylene Carbonate Under Continuous DC Electric Field using Kerr Effect

Z. N. Zakaria\*, M. S. Laili\*, N. A. Rahman\*, P. L. Lewin\*\*, T. Andritsch\*\*, and N. Hussin\*(C.A.)

**Abstract:** The study investigates the electric field and space charge distributions in propylene carbonate under direct current (DC) applied fields using Kerr effect. Propylene carbonate is known for its high permittivity and is utilised in many applications, including electrochemical systems and dielectric materials. Understanding the behaviour of electric fields and space charge distributions within propylene carbonate is critical for optimising its performance in these applications. In the study, Kerr effect is employed which by applying the DC electric field across the test liquid for measuring the electric field and space charge distributions within the propylene carbonate. The experimental setup involved a controlled application of DC fields, and the Kerr effect measurements were conducted using an optical system. The results show significant understandings into the behaviour of space charges and their influence on the electric field distribution in propylene carbonate. Distinct patterns of charge accumulation and electric field distortion were observed and analysed in the dielectric liquid properties and charge transport mechanisms. The relationship between electric fields and space charges in propylene carbonate under DC conditions has been provided by the findings. The study also shows that the Kerr effect is a useful tool for studying electric field distributions in complex materials.

**Keywords:** Electric field, Space charge, Kerr effect, Propylene carbonate, Dielectric liquid

## 1 Introduction

THE investigation of electric fields and space charge dynamics in dielectric materials is crucial for advancing our understanding in the electrical insulation of power apparatus. Space charge in dielectric liquids can be generated due to charge injection from electrodes or ionisation of impurities and molecules within the liquid [1], [2]. These space charges distort the electric field distribution and can affect the performance and

reliability of the dielectric materials. Therefore, a study of electric field and space charge distribution in dielectric liquids is important for improving the effectiveness of electrical insulation in high-voltage equipment.

The Kerr effect provides a powerful and sensitive method for quantifying the electric field distribution and space charge behaviour within propylene carbonate [3]-[8]. When a DC electric field is applied to propylene carbonate, the resulting birefringence can be measured to infer the magnitude and spatial distribution of the electric field. This non-invasive optical technique allows for precise measurements without disrupting the system under study. Through comprehensive experimental analysis, the investigation on continuous DC electric fields influences the formation and migration of space charges in propylene carbonate.

Liquids like nitrobenzene [9], [10], purified water [11], transformer oil [12], [13] and propylene carbonate [14],

Iranian Journal of Electrical & Electronic Engineering, 2025.

Paper first received 31 Dec 2024 and accepted 22 Feb 2025.

\* The author is with the Faculty of Electrical Engineering & Technology, Universiti Malaysia Perlis, Malaysia.

E-mail: [nuriziani@unimap.edu.my](mailto:nuriziani@unimap.edu.my).

\*\* The authors are with the School of Electronics and Computer Science, University of Southampton, United Kingdom.

Corresponding Author: N. Hussin.

[15] exhibit the Kerr effect and have been used in measurements. Unlike the transformer oil which has a Kerr constant of  $B \sim 10^{-15} \text{ mV}^{-2}$ , propylene carbonate exhibits a significantly higher Kerr constant of  $B \sim 10^{-12} \text{ mV}^{-2}$ . This significant difference allows the Kerr effect to be observed at much lower electric fields, making propylene carbonate a suitable test liquid for Kerr electro-optic investigations. Furthermore, its non-toxic nature further enhances its suitability for experimental applications, providing both safety and reliability in laboratory settings.

Most studies have focused on the application of high impulse voltages in measuring electric field and space charge distributions in dielectric liquids using Kerr effect [10], [14]-[16]. While DC field is less commonly applied than impulse, DC electric field measurement can provide complementary information about the dielectric behaviour of the dielectric liquid under steady-state conditions. Maeno et.al [17] in their study has developed a voltage modulation based on the Kerr electro-optic technique specifically to measure the DC electric field strength in low Kerr constant liquid like the transformer oil. However, this technique depends on the AC modulation and utilises elliptically polarised light with a small retardation angle. Due to its complexity to the setup and may require precise calibration and control, this technique is less straightforward compared to other measurement techniques.

The investigation of electric field measurements in dielectric liquids, particularly at low DC levels presents a challenge for understanding the fundamental of electrical properties. This is because under long applied high DC electric field, the measurement can be affected by heating the liquid and may also produce electroconvection [18]. X. Zhang et.al [18] in his study reported that when there is high enough DC voltage applied to the transformer oil, the turbulence of electroconvection is observed. That phenomena could then affect the electric conduction in the liquid.

Hence, this study employed the Kerr effect measurements in propylene carbonate under low applied DC electric fields ( $E < 2.86 \text{ kV/mm}$ ) to minimise the temperature rising and the electroconvection effect. This paper aims to investigate the complex relationship between electric field and space charge effect in propylene carbonate under continuous DC electric fields using Kerr effect method. A parallel electrode is employed with gap of  $d = 2.1 \text{ mm}$  and the length of the electrode,  $L$  is  $80 \text{ mm}$ . By applying continuous low voltage to the propylene carbonate, the behaviour of the spatial charge at certain electric field is investigated.

### 1.1 Principle of Kerr Effect

In general, most dielectric materials are isotropic.

However, if subjected to external force like electric field, the material becomes anisotropic. Fig. 1 shows a linearly polarised incident light propagates along the  $z$  direction, where the anisotropic dielectric exhibits birefringence along the  $x$  and  $y$  directions. Due to the birefringence, the electric field component of  $e_{x1}$  and  $e_{y1}$  of the light propagate at slightly different velocities where  $x$  direction is a slow axis and the  $y$  direction is a fast axis. Therefore, after the light passed through the dielectric material, an optical phase retardation  $\phi$  is produced. If the direction of the fast axis of the birefringence keeps constant along the light path, the produced optical phase retardation  $\phi$  is given as,

$$\phi = \frac{2\pi}{\lambda_0} (n_x - n_y)L \quad (1)$$

Where  $\lambda_0$  is the wavelength of the light in space,  $L$  is the optical path length and  $\Delta n$  is the refractive index difference between  $n_x$  and  $n_y$  in the dielectric material.

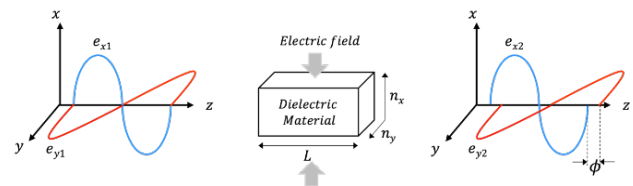


Fig. 1 Optical phase retardation caused by a birefringence [19]

Kerr effect is an electro-optical effect that was first observed by John Kerr in 1877. Under high electric fields, a dielectric liquid become birefringent, or the refractive index of the liquid changes when high electric field,  $E$  is applied. The difference in refractive indices can be determined by measuring the resultant optical phase shift,  $\phi$  that is given by:

$$\phi = 2\pi BLE^2 \quad (2)$$

Where  $B$  is the Kerr constant of the liquid material. Generally, it is difficult to measure the optical phase shift directly. However, it can be determined from the measurement of light intensity of the transmitted light through the dielectric material. The relationship between the transmitted light intensity,  $I$  and the optical phase shift is given by [20],

$$I = I_m \sin^2 \left[ \frac{\phi}{2} \right] \quad (3)$$

and the relationship of the transmitted light intensity as a function of electric field is as follows.

$$I = I_m \sin^2 \left[ \frac{\pi}{2} \left( \frac{E}{E_m} \right)^2 \right] \text{ where, } E_m = \frac{1}{\sqrt{2BL}} \quad (4)$$

$I_m$  is the magnitude of the maximum incident light,  $E_m$  is magnitude of the necessary electric field to reach the first maximum light intensity.

## 1.2 Electric Field

Preferably, the electric field between two electrodes will produce same distribution of field. But, in dielectric liquid, the asymmetric electric field distribution is produced. There are two factors that contribute to electric field distribution in liquids. As illustrated in Fig. 1, the voltage applied,  $V$  to the electrodes is given by,

$$V = \int_0^d E(x, z) dx \quad (5)$$

Where  $d$  is the gap distance between the parallel electrodes. Hence, the integral of the electric field  $E(x, z)$  over the distance  $d$  must equal the applied voltage  $V$ . Besides, according to Poisson's equation, space charge distorts the electric field distribution in dielectric liquid. The relationship of the Poisson's equation that relates the electric field to the charge density,  $\rho$  as in Equation (6).

$$\nabla \cdot E = \frac{\rho}{\epsilon} \quad (6)$$

By symmetry and assuming a linear, isotropic medium, the problem simplifies to considering variations only along the x-axis. As the investigation considers one-dimensional form, assumptions are made. Firstly, the system is assumed to be symmetric with respect to the z-axis. This means the properties of the material and the distribution of the electric field and space charge are uniform in the z-direction. Thus, the electric field,  $E$  and space charge density,  $\rho$  can be considered functions of  $x$  alone. Secondly, in a linear isotropic medium, the relationship between the electric field,  $E$  and the displacement field,  $D$  is given by  $D = \epsilon E$ , where  $\epsilon$  is the permittivity of the liquid. Furthermore, an isotropic medium has uniform material properties in all directions, ensuring that  $\epsilon$  is a constant scalar value and not a direction-dependent [19]. Given these assumptions, the space charge density  $\rho$  can only vary with x-axis, leading to the simplified form of Poisson's equation as follows.

$$\rho(x) = \epsilon_0 \epsilon_r \frac{dE_x}{dx} \quad (7)$$

If there is no space charge between the electrodes,  $dE_x/dx$  is zero and the electric field is uniform. However, when the electric field is not constant, it means that the electric field varies with the position along the x-axis. This

variation in the electric field is often due to the presence of space charges [21]. Hence, the electric field distribution across the electrodes can be determined by reducing Equation (4) as follows.

$$\left(\frac{E}{E_m}\right)^2 = \frac{2}{\pi} \sin^{-1} \left( \sqrt{\frac{I}{I_m}} \right) \quad (8)$$

## 2 Methodology

### 2.1 Experimental Setup

The experimental setup for investigating the Kerr effect in propylene carbonate under a DC electric field is demonstrated in Fig. 2. A 7 mW Helium-Neon laser is employed as the coherent light source. The laser beam is initially expanded using a beam expander to increase its diameter, ensuring uniformity and reducing beam divergence. The expanded beam then passes through a lens, which focuses the light through the propylene carbonate. As the laser beam passes the propylene carbonate, the electric field induces birefringence and alters the polarisation state of the transmitted light. To detect these changes, a polariser and analyser is set to  $+45^\circ$  and  $-45^\circ$  respectively and followed by a photodetector and a camera.

In the study, the Kerr experimental setup includes both a photodiode and a camera, enabling simultaneous measurements for enhanced accuracy and comparative analysis. The photodetector captures the intensity variations of the transmitted light, which are directly related to the electric field-induced and the camera records the spatial change of the light intensity under the field stress in the propylene carbonate. A beam splitter is used to split the output light into two beams while a lens is used to focus the output light onto both the photodiode and the camera. All optical components are fixed on to an optical bench and covered with an enclosure to minimise background noise. Electrodes are immersed in the propylene carbonate liquid sample and connected to a DC power supply, enabling the application of a controlled electric field across the sample. In this study, the DC voltage ranges from 0.1 kV to 6 kV were applied continuously to the system across the electrode gap of 2.1 mm. Each measurement was taken every 2 minutes. Fig. 2(a) depicts a schematic diagram showing the configuration and key components, and Fig. 2(b) shows the practical arrangement within the designated laboratory environment.

### 2.2 Electric Field Measurement

The flowchart in Fig. 3 outlines a systematic procedure for determining the electric field and calculating the

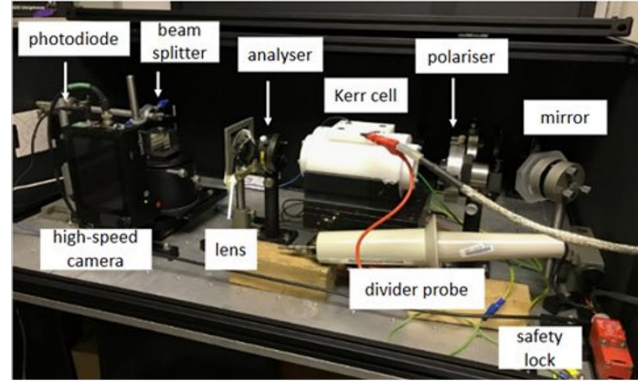
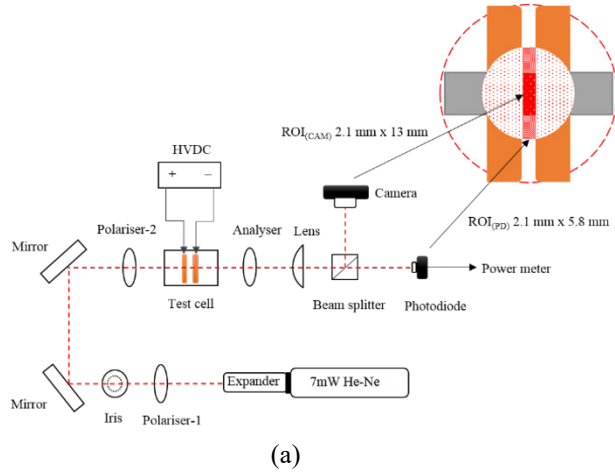


**Fig. 2** Kerr experimental setup with photodiode and camera (a) in schematic diagram and (b) in designated laboratory

space charge in propylene carbonate under a DC electric field. The process begins with the initial input of data, including parameters such as the propylene carbonate Kerr constant  $B$ , the optical path length  $L$ , and the gap size  $d$ . The first step involves determining the maximum electric field  $E_m$ . Subsequently, the recorded images are loaded and read. These images are converted from RGB to grayscale to simplify the subsequent analysis. An image filtering step is applied to enhance the quality and clarity of the grayscale images, making it easier to identify relevant features. The next step involves defining the edges of the electrodes within the images to establish the regions of interest (ROI) for the analysis.

Once the ROI is defined, the electric field across the sample is determined. This involves calculating the field distribution using the known electrode geometry and applied voltage. The integral of the electric field is checked to ensure that the applied voltage matches the expected electric field average values. If the condition is not satisfied, adjustments are made, and the electric field determination is repeated. Once the electric field is accurately determined, the charge density is calculated.

This involves using the electric field results and solving Poisson's equation to obtain the spatial distribution of the space charge within the sample. The results of these calculations, including the electric field and charge density distributions, are plotted for analysis. The process concludes with a comprehensive plotting of the results, which provides understandings into the behaviour of the electric field and space charge within the propylene carbonate under the applied DC electric field. This structured approach ensures accurate and reliable determination of electro-optical properties essential for understanding the Kerr effect in propylene carbonate.

### 3 Results

#### 3.1 Light Intensity Relative to Electric Field

According to Malus's law, the light intensity transmitted,  $I$  by the analyser is proportional to the square of cosine of the angle,  $\theta$  between the polariser and the analyser [22]. This is conceptually similar to the Kerr effect light intensity ratio,  $I/I_m$  where,  $\cos^2(\theta) = \sin^2(\pi BLE^2)$ . When  $\theta = 0$ , maximum light transmission passes through the analyser, thus  $\sin^2(\pi BLE^2) = 1$ . While when  $\theta = \frac{\pi}{2}$ , no light can be transmitted through the analyser, hence  $\sin^2(\pi BLE^2) = 0$ . This concept is similar to the configuration of crossed linear polariscope setups used in Kerr effect measurement. In both cases, the arrangement of optical components allows for the detection of changes in light polarisation caused by the electric field.

Fig. 4 shows the measurement of the light intensity ratio as a function of electric field in propylene carbonate. From the measurement results, it is observed that some light was detected when no electric field is applied. The measurement was considered to include background noises that cannot be eliminated. Therefore, Equation (2) can be written as,

$$\frac{I}{I_m} = \sin^2(\pi BLE^2) + C \quad (9)$$

Where  $C$  is a constant. If noise is considered in the measurement, the light intensity ratio can be expressed as follows.

$$\frac{I}{I_m} = \begin{cases} 1 + C & \text{when } \theta = 0, I = I_m \\ C & \text{when } \theta = \frac{\pi}{2}, I = I_{noise} \end{cases} \quad (10)$$

By substituting Equation (9) into Equation (10), the measurement can be corrected by deducing the

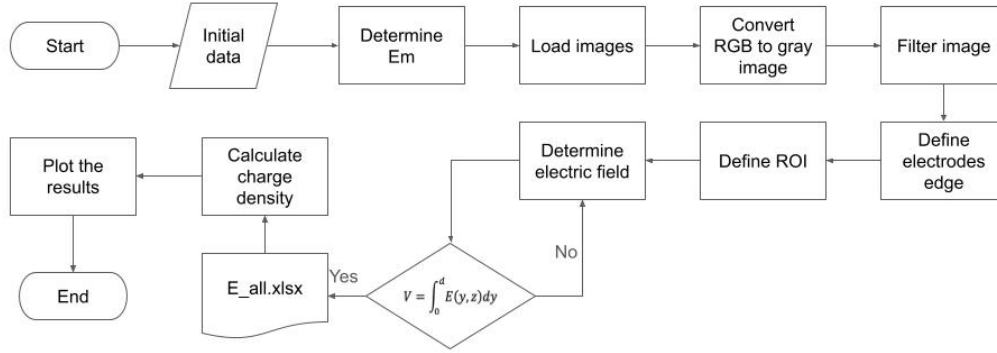


Fig. 3 Workflow for determining electric field and space charge distribution

background noise from the noisy measurement reading as shown below.

$$\frac{I - I_{noise}}{I_m - I_{noise}} = \sin^2(\pi BLE^2) \quad (11)$$

As depicted in Fig. 4, in the absence of an electric field, the light intensity before correction shows a certain value, as marked by the red indicator, while the corrected light intensity is observed to be zero. This initial intensity, due to background noise or other factors, is subtracted during the correction process. From the results, it is evident that as the applied electric field increases, the transmitted light intensity also increases, eventually reaching a maximum value. This trend demonstrates the relationship between the electric field strength and the Kerr effect in propylene carbonate, where the light intensity reaches its peak once the field intensity surpasses the required electric field intensity,  $E_m$ .

### 3.2 Kerr Constant

Kerr constant of propylene carbonate can be determined from the light intensity measurement. From Equation (3), it shows that phase-shift  $\phi$  is directly proportional to the square of the applied electric field. Therefore, from Equation (4), the Kerr constant B can be calculated using the slope of the square of applied voltage as a function of phase shift. Thus, Equation (4) can be rearranged as follows.

$$V^2 = \frac{d^2}{\pi BL} \sin^{-1} \left( \sqrt{\frac{I}{I_m}} \right) \quad (12)$$

Fig. 5 shows the linear regression analysis of the square of applied voltage relative to the phase shift from the light intensity measurement in propylene carbonate. Given the slope is 106419, the electrode gap,  $d = 2.1$  mm and the optical length,  $L = 80$  mm, Kerr constant of the propylene carbonate is determined,  $B = 1.41 \times 10^{-12}$  mV<sup>-2</sup>

based Equation (12). Consequently, the necessary electric field magnitude,  $E_m$  at the first light maxima is observed to be 2.11 kVmm<sup>-1</sup> using the expression  $(\sqrt{2BL})^{-1}$ , that is also demonstrated in Fig. 4.

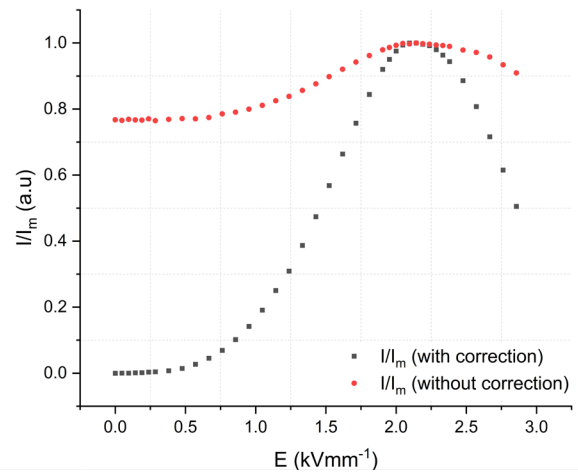


Fig. 4 Correction of the light intensity ratio relative to electric fields in propylene carbonate

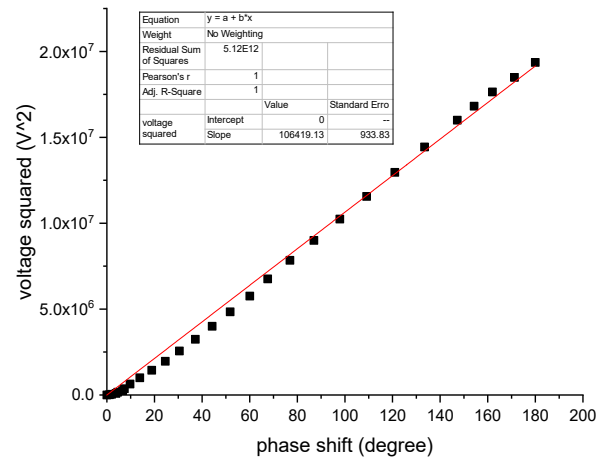


Fig. 5 Square of applied voltage as a function of the phase shift

### 3.3 Electric Field and Space Charge Distributions

Fig. 6 shows the electric field and charge density distributions in propylene carbonate under various DC electric fields, with 0 mm denoting the region near the anode and 2.1 mm indicating the region near the cathode. The electric field distribution within the electrode gap with various applied electric fields is shown in Fig. 6(a). For lower applied fields,  $0.24 \text{ kVmm}^{-1}$  and  $0.47 \text{ kVmm}^{-1}$  the electric field distribution is relatively almost uniform across the gap. This suggests minimal variation in the electric field strength throughout the distance between the electrodes.

As the applied electric field strength increases at  $0.96 \text{ kVmm}^{-1}$ ,  $1.43 \text{ kVmm}^{-1}$ ,  $1.90 \text{ kVmm}^{-1}$ ,  $2.38 \text{ kVmm}^{-1}$  and  $2.86 \text{ kVmm}^{-1}$ , a more pronounced distribution is observed. The non-uniformity in the electric field distribution at higher applied fields corresponded to the accumulation of space charges within the propylene carbonate. These charges modify the local electric field, forming regions of higher and lower field strengths. For example, at the applied field of  $2.38 \text{ kVmm}^{-1}$ , the electric field distribution exhibits the most significant variation with a pronounced peak. This indicates that the space charge effect is most prominent under this condition. In contrast, at the lowest applied field of  $0.24 \text{ kVmm}^{-1}$ , the electric field distribution is less distorted, indicating that space charge effects are minimal or negligible at this field strength.

Fig. 6(b) shows the charge density distribution in propylene carbonate between electrodes under various DC electric fields. At lower applied fields of  $0.24 \text{ kVmm}^{-1}$  and  $0.47 \text{ kVmm}^{-1}$ , the charge density remains nearly constant and close to zero across the electrode gap, indicating minimal charge accumulation. However, as the applied electric field increases from  $0.95 \text{ kVmm}^{-1}$  to  $2.86 \text{ kVmm}^{-1}$ , the charge density distribution exhibits significant variations, with pronounced peaks indicating strong charge accumulation and separation within the gap. The presence of both positive and negative peaks suggests that space charges are accumulating near one electrode and depleting near the other, leading to charge separation. For example, the results in Fig. 6(b) indicates that the maximum positive and negative charge densities near the anode occur at  $2.38 \text{ kVmm}^{-1}$  and  $0.95 \text{ kVmm}^{-1}$ , respectively. In contrast, the maximum positive and negative charge densities near the cathode are found at  $2.86 \text{ kVmm}^{-1}$  and  $2.36 \text{ kVmm}^{-1}$ , respectively.

In summary, these charge density variations are crucial for understanding the behaviour of under DC electric fields. The accumulation and separation of space charges can significantly influence the dielectric liquid properties and local electric fields. As more electric fields are

applied, more significant changes in charge density are observed. This condition highlights the significant impact of strong space charge effect. These effects are directly related to the Kerr effect measurements, as the local field variations caused by space charges will exhibit changes in birefringence. Understanding these distributions helps in predicting and analysing the Kerr effect response in other dielectric liquid.

### 3.4 Charge Density

Fig. 7 shows the charge density  $\rho$  as a function of the applied electric field  $E$  in the propylene carbonate. The data points represent measurements taken at different positions relative to the electrodes: near the anode at  $d = 0.1 \text{ mm}$ , at the middle of the electrode gap  $d = 1.05 \text{ mm}$  and near the cathode at  $d = 2.0 \text{ mm}$ . The results demonstrate the spatial distribution of charge density  $\rho$  in propylene carbonate under varying applied electric fields. At the middle of electrodes,  $d = 1.05 \text{ mm}$  the charge density remains relatively stable and close to zero, indicating minimal space charge accumulation in these regions. This distribution suggests that at the midpoint, the propylene carbonate maintains a balanced charge distribution, likely due to the effective neutralisation and redistribution of charges by the electrode surfaces.

In contrast, the measurements taken near the anode and cathode show more significant variations in charge density, with distinct positive and negative density. From the result, it can be observed that the charge density ranges from approximately  $-0.6 \text{ Cm}^{-3}$  at the  $0.95 \text{ kVmm}^{-1}$  to  $+0.4 \text{ Cm}^{-3}$  at  $2.38 \text{ kVmm}^{-1}$ . Whilst, near cathode at  $d = 2.0 \text{ mm}$ , the charge density shows more noticeable variations. For instance, at an applied electric field of  $2.38 \text{ kVmm}^{-1}$ , the charge density reaches  $-1.1 \text{ Cm}^{-3}$ . While the at  $2.86 \text{ kVmm}^{-1}$ , the charge density  $0.2 \text{ Cm}^{-3}$  is observed.

This increased variation indicates that space charge effects are more pronounced in regions further from the electrodes. There are possibly two significant factors that caused the fluctuation of change density in the propylene carbonate. Field distortion within the electrodes is observed which lead to higher or lower field strength near the electrodes. It is known that more space charge has accumulated near the electrodes. Furthermore, the mobility of ions or charged particles in the propylene carbonate might cause the drifting and the accumulation near the electrodes especially under the influence of a continuous DC electric fields. Hence, the nonuniform electric field here could lead to localised charge accumulation, making these areas more sensitive to changes in the applied electric field.



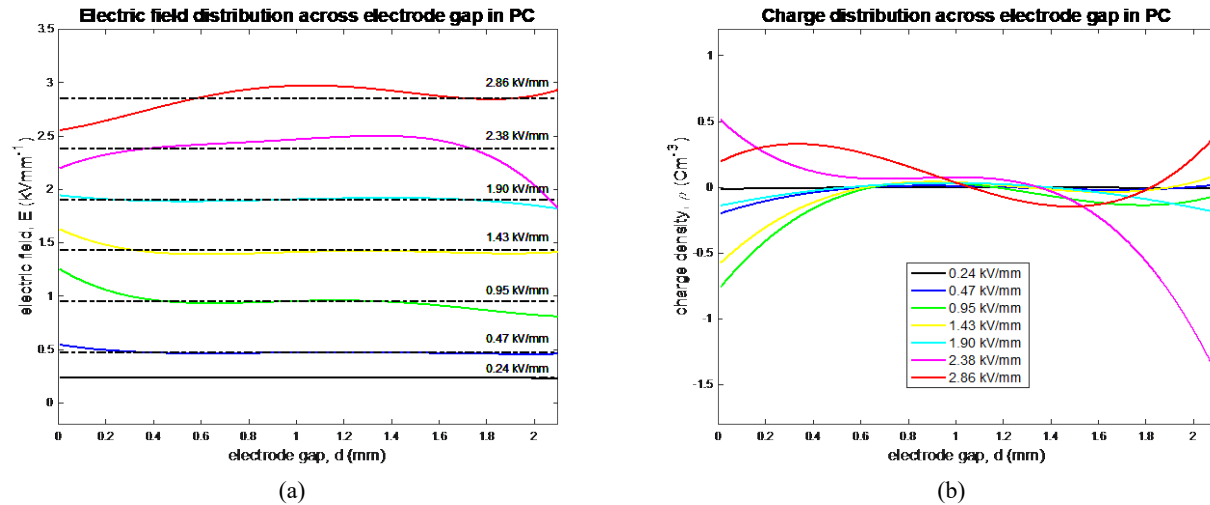


Fig. 6 (a) Electric field and (b) charge density distributions between the electrode gap in propylene carbonate

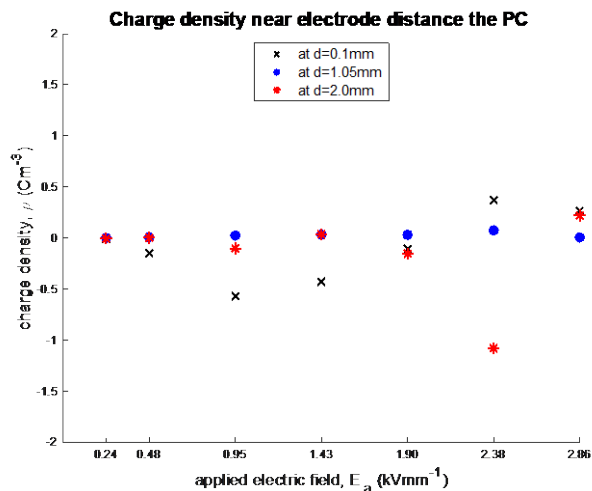


Fig. 7 Charge density near anode ( $d = 0.1$  mm), mid electrode ( $d = 1.05$  mm) and near cathode ( $d = 2.0$  mm)

#### 4 Conclusions

In this study, the relationship between space charge accumulation and electric field distribution in propylene carbonate under continuous DC electric fields using the Kerr effect has been investigated. The experiments demonstrated that the Kerr effect is a great method for measuring electric fields and space charge dynamics in dielectric materials without direct interference. As the voltage increased, the results showed an increase of electric field distortions within the liquid. Hence, the findings revealed a strong correlation between the applied electric field and space charge distribution in propylene carbonate.

As the electric field increases, the movement of charge near electrodes is observed. The results showed that middle of the electrode, minimal charge density is

observed. In the other hand, charges near anode and cathode have shown variation of density. This is highly due to the distribution of charges at the electrodes, thus influences the electric field distribution in propylene carbonate.

These results have significant implications for the design and optimization of electro-optical devices and energy storage systems. Understanding the relationship between space charge and electric fields in propylene carbonate can lead to improved performance and reliability of devices that utilize this material. Additionally, the study can be applied to other dielectric materials, broadening the scope of its applicability.

#### Acknowledgment

This research was funded by a grant from Ministry of Higher Education of Malaysia (FRGS/1/2023/TK09/UNIMAP/03/1).

#### References

- [1] M. Zahn, 'Space charge effects in dielectric liquids', in *The Liquid State and Its Electrical Properties*, vol. 193, Springer US, 1988, pp. 367–430.
- [2] T. J. Lewis, 'Basic electrical processes in dielectric liquids', *IEEE Transactions on Dielectrics and Electrical Insulation*, vol. 1, no. 4, pp. 630–643, 1994, doi: 10.1109/94.311706.
- [3] T. J. Gung, A. Ustundag, and M. Zahn, 'Preliminary Kerr Electro-Optic Field Mapping Measurements in Propylene Carbonate Using Point-Plane Electrodes', *J Electrostat*, vol. 3886, no. 99, pp. 79–89, 1999.
- [4] J. Shi, Q. Yang, W. Sima, L. Liao, S. Huang, and M. Zahn, 'Space charge dynamics investigation based on Kerr electro-optic measurements and

- processing of CCD images', IEEE Transactions on Dielectrics and Electrical Insulation, vol. 20, no. 2, pp. 601–611, 2013, doi: 10.1109/TDEI.2013.6508764.
- [5] Z. Zhang, S. Wu, W. He, and Q. Yang, "A Novel Transient Electric Field Measurement for Low Kerr Constant Liquid Dielectrics Based on Concave Spherical Mirror Conjugate Structure," IEEE Transactions Instrumentation and Measurement, 2023, doi: 10.1109/TIM.2022.3225024.
- [6] H. Ihuri, S. Ninomiya, and M. Fujii, 'Optical measurement of electric field distributions with time in propylene carbonate', Electronics and Communications in Japan, vol. 94, no. 9, pp. 45–51, 2011, doi: 10.1002/ecj.10351.
- [7] Z. N. Zakaria, T. Andritsch, and P. L. Lewin, 'Kerr Measurement Approaches in Propylene Carbonate under DC Electric Field', IEEE 2nd International Conference on Dielectrics, ICD 2018, pp. 1–4, 2018, doi: 10.1109/ICD.2018.8468415.
- [8] Z. N. Zakaria, P. L. Lewin, and T. Andritsch, 'Light Intensity Measurement of Kerr Effect Using Photodiode and High-Speed Camera in Propylene Carbonate under Applied DC Electric Fields', J Phys Conf Ser, vol. 1878, no. 1, pp. 0–9, 2021, doi: 10.1088/1742-6596/1878/1/012044.
- [9] A. W. Bright, B. Makin, and A. J. Pearmain, 'Field distribution in nitrobenzene using the Kerr effect', J Phys D Appl Phys, vol. 2, no. 3, p. 447, 1969, [Online]. Available: <http://iopscience.iop.org/0022-3727/2/3/319>
- [10] E. C. Cassidy, R. E. Hebner, M. Zahn, and R. J. Sojka, 'Kerr-effect studies of an insulating liquid under varied high-voltage conditions', IEEE Transactions on Electrical Insulation, vol. EI-9, no. 2, pp. 43–56, 1974, doi: 10.1109/TEI.1974.299310.
- [11] M. Zahn and T. Takada, 'High voltage electric field and space-charge distributions in highly purified water', J Appl Phys, vol. 54, no. 9, pp. 4762–4775, 1983, doi: 10.1063/1.332810.
- [12] X. Zhang and M. Zahn, 'Kerr electro-optic field mapping study of the effect of charge injection on the impulse breakdown strength of transformer oil', Appl Phys Lett, vol. 103, no. 16, p. 162906, 2013, doi: 10.1063/1.4826185.
- [13] K. Tanaka and T. Takada, 'Measurement of the 2-Dimensional Electric Field Vector in Dielectric Liquids', IEEE Transactions on Dielectrics and Electrical Insulation, vol. 1, no. 4, pp. 747–753, 1994, doi: 10.1109/94.311720.
- [14] A. Helgeson and M. Zahn, 'Kerr electro-optic measurements of space charge effects in HV pulsed propylene carbonate', IEEE Transactions on Dielectrics and Electrical Insulation, vol. 9, no. 5, pp. 838–844, 2002, doi: 10.1109/TDEI.2002.1038666.
- [15] W. Sima, Q. Chen, P. Sun, M. Yang, H. Guo, and L. Ye, 'Asymmetric injection and distribution of space charges in propylene carbonate under impulse voltage', J Phys D Appl Phys, vol. 51, no. 21, 2018, doi: 10.1088/1361-6463/aab99c.
- [16] Z. Zhang, Q. Yang, S. Wu, and W. He, 'Temperature Effect on Dielectric Properties of Propylene Carbonate under Switching Overvoltage', IEEE Transactions on Dielectrics and Electrical Insulation, vol. 29, no. 2, pp. 428–436, Apr. 2022, doi: 10.1109/TDEI.2022.3157934.
- [17] T. Maeno, Y. Nonaka, and T. Takada, 'Determination of Electric Field Distribution in Oil using the Kerr-effect Technique after Application of dc Voltage', IEEE Transactions on Electrical Insulation, vol. 25, no. 3, pp. 475–480, 1990, doi: 10.1109/14.55719.
- [18] X. Zhang, 'Electro-optic signatures of turbulent electroconvection in dielectric liquids', Appl Phys Lett, vol. 104, no. 20, May 2014, doi: 10.1063/1.4879280.
- [19] T. Takada, 'Acoustic and optical methods for measuring electric charge distributions in dielectrics', IEEE Transactions on Dielectrics and Electrical Insulation, vol. 6, no. 5, pp. 519–547, 1999, doi: 10.1109/CEIDP.1999.804581.
- [20] M. Zahn, 'Transform Relationship between Kerr-effect Optical Phase Shift and Nonuniform Electric Field Distributions', IEEE Transactions on Dielectrics and Electrical Insulation, vol. 1, no. 2, pp. 235–246, 1994, doi: 10.1109/94.300256.
- [21] R. Tobazeon, M. Haidara, and P. Atten, 'Ion injection and Kerr plots in liquids with blade-plane electrodes', J Phys D Appl Phys, vol. 17, no. 6, pp. 1293–1301, 1984, doi: 10.1088/0022-3727/17/6/025.
- [22] E. Collet, Field Guide to Polarization. Bellingham, WA: SPIE Press, 2005.



**Paul L. Lewin** was born in Ilford, Essex in 1964. He received the BSc (Hons) and PhD degrees in electrical engineering from the University of Southampton, UK in 1986 and 1994, respectively. He joined the academic staff of the University in 1989 and is Professor of Electrical Power Engineering and Head of

Electronics and Computer Science, where he is also the Director of the Tony Davies High Voltage Laboratory. His research interests are within the generic areas of applied signal processing and control. Within high voltage



engineering this includes condition monitoring of HV cables and plant, surface charge measurement, HV insulation/dielectric materials and applied signal processing. In the area of automation, he is particularly interested in the practical application of repetitive control and iterative learning control algorithms.



**Thomas Andritsch** received the Dipl.-Ing. Degree in Electrical Engineering from Graz University of Technology in 2006 and his Ph.D. degree in the same field from Delft University of Technology in 2010. He is currently working as an Associate Professor at the University of Southampton with focus on

advanced materials for high voltage applications and plant. He has extensive experience with preparation and testing of polymer-based electrical insulation materials, including nanodielectrics, electroactive polymers and syntactic foams, as well as liquid insulation systems and nanofluids.



**Nuriziani Hussin**, born in 1984 in Pahang, Malaysia, is an Associate Professor at the Faculty of Electrical Engineering & Technology, Universiti Malaysia Perlis (UniMAP). She earned her Bachelor of Science (Hons) and PhD degrees in Electrical Engineering from the University of Southampton, UK, in

2007 and 2011, respectively. Since joining UniMAP in 2011, Dr. Hussin has specialized in high voltage insulation and measurement, lightning protection, and grounding systems. Her research contributions include studies on the effects of nanoparticles and antioxidants on natural oil performance in high voltage applications and the influence of lightning and grounding conditions on flashover events in transmission lines. Dr. Hussin is also a member of the Malaysian High Voltage Network (MyHVnet), an organization dedicated to advancing high voltage engineering research and development.



**Muhammad Shakir Laili** was born on January, 1982, in Kuala Lumpur, Malaysia. He completed his Bachelor in Electrical Engineering in 2007 and his Master in Power Electrical Engineering in 2009, both from Universiti Teknologi Malaysia (UTM). Currently, he serves as a lecturer at the Faculty of Electrical

Engineering & Technology at Universiti Malaysia Perlis (UniMAP). His research interests are concentrated in the field of high voltage engineering. This includes the calibration of high voltage equipment, condition monitoring of high voltage cables, high voltage insulation and dielectric materials, and applied signal processing.



**Norjasmi Abdul Rahman** was born in Beseri, Perlis, Malaysia, in July 1980, is a lecturer at the Faculty of Electrical Technology & Engineering, University Malaysia Perlis (UniMAP), where he has been since 2010. He holds a Bachelor of Engineering (Hons) in Industrial Electronic Engineering from Universiti Malaysia Perlis (2007) and a Master of Engineering in Electrical & Electronic Engineering from Aalto University, Finland (2010). Currently pursuing a Ph.D. in Power Electronics, his research interests include power electronic converters, photovoltaic systems, renewable energy systems, and high voltage technologies.



**Zetty Nurazlinda Zakaria** was born in Negeri Sembilan, Malaysia in January 1983, and is a lecturer at the Faculty of Electrical Technology & Engineering, University Malaysia Perlis (UniMAP), where she has been since 2010. She received her Bachelor degree (2006) and Master degree (2009) from Universiti Teknologi Malaysia, Johor, both in the field of

electrical engineering. Currently pursuing a Ph.D. in liquid insulation. Her research interests focus on insulation in high voltage systems, lightning phenomena and power system analysis.

